EXAMINATION OF UNCONTROLLED MASS PER YEAR AS AN ENVIRONMENTAL INDEX

Dominick G. Bologna(1), Gregory A. Henning(2), Marlon E. Sorge(2), Juan C. Maldonado(1), Lily Wahleithner(1), Victor H. Cabrera(1)

(1) The Aerospace Corporation, 2310 E. El Segundo Blvd, El Segundo, CA 90245, USA, Emails: dominick.g.bologna@aero.org, juan.c.maldonado@aero.org, lily.wahleithner@aero.org, victor.h.cabrera@aero.org
(2) The Aerospace Corporation, 2155 Louisiana Blvd. #5000, Albuquerque, NM 87110, USA Emails: gregory.a.henning@aero.org, marlon.e.sorge@aero.org

ABSTRACT

The Aerospace Corporation's Aerospace Debris Environment Projection Tool (ADEPT) models the evolution of the on-orbit debris environment based on different levels of space traffic and debris mitigation practices. ADEPT's unique modeling process allows for hundreds of future environment simulations to be run simultaneously. In 2019, Uncontrolled Mass per Year (UMPY) was developed to characterize the "level of activity" exhibited across these simulations and evaluate how certain behaviors might influence the future debris environment. Since then, UMPY has undergone multiple changes to improve the correlation between operational behaviors and their environmental impacts.

This work explores the process of designing the UMPY index, starting from its initial implementation. The decision to use mass and lifetime as proxies for collision severity and risk comes after testing the use of other object parameters, including cross-sectional area and altitude. Later changes were made to better account for the environmental impact of successfully disposed objects and the non-linear effect of lifetime on collision probability. Results from over one thousand ADEPT simulations are used to compare how well different UMPY formulations correlate to different environmental metrics. Other commercial indices are also examined and compared to UMPY.

1 INTRODUCTION

Space activity has experienced significant growth over the past few years, driven by increasingly affordable access to Low-Earth Orbit. In response, new debris mitigation and space traffic management initiatives have been developed by multiple organizations worldwide. Evaluating these new propositions requires metrics to quantify their potential effectiveness; one approach is to directly use information present in observed or simulated data, such as object count or on-orbit mass. A more nuanced approach is to use an environmental index that simultaneously incorporates multiple aspects of the debris environment through a combination of various spacecraft, mission, and environmental parameters. Dozens of such indices have been published, each focused on different aspects of the space debris environment. Some characterize the stability of the environment [1] while others address the environmental risks posed by specific missions [2] or derelict objects [3,4].

One such environmental index is Uncontrolled Mass per Year (UMPY). UMPY was developed as a simple way to characterize and compare the results of future environment simulations. Previous studies [5,6,7,8,9] have shown strong correlations between UMPY and various environmental metrics, including population growth, collision rates, and conjunction frequencies. Through these correlations, UMPY can be used to predict how certain behaviors, such as post-mission disposal methods, might influence the future debris environment without the use of simulations. Furthermore, UMPY could serve as a target threshold for specific operators to ensure sustainable space operations.

UMPY has evolved since its introduction in 2019 [5]. This work explains each design decision made when developing UMPY, starting with the initial parameter selection process. This work uses simulation results from The Aerospace Corporation's Aerospace Debris Environment Projection Tool (ADEPT), which has previously been used to inform U.S. and International Space Traffic Management and debris mitigation policy. The results from over one thousand future environment simulations are used to determine how well each formulation correlates to different environmental metrics. Furthermore, two simple regulatory metrics and one orbital capacity index are studied to evaluate how effective each is relative to the simulation results.

2 AEROSPACE DEBRIS ENVIRONMENT PROJECTION TOOL

The ADEPT simulation process generates representations of the future on-orbit environment using a population model containing mass, size, and trajectory data for a complete set of Earth orbiting objects. Early versions of ADEPT are described in [10] and [11]. Recent enhancements to the Monte Carlo processing loop and details regarding the different components and flow of ADEPT are described in [7] and [12]. In brief:

Proc. 9th European Conference on Space Debris, Bonn, Germany, 1–4 April 2025, published by the ESA Space Debris Office
Editors: S. Lemmens, T. Flohrer & F. Schmitz, (http://conference.sdo.esoc.esa.int, April 2025)

1. An initial population model (IPM) is generated, containing known catalog objects and a future launch model (FLM).
2. IPM object ephemerides are generated by the long-term, Draper Semi-Analytic mean-element propagator MEANPROP [13].
3. Future collisions are generated based on collision probability calculations from an orbit trace crossing method (OTC) [14].
4. The fragmentation modeling code IMPACT [15] is used to generate fragments from collisions and explosions.
5. Fragments are fed back into the process as step 2 to produce multiple generations of collisions and debris.

Each pass through the ADEPT process produces a new generation of fragmentation debris. When a new generation of debris is fed back into the cycle, they interact with all other objects from previous generations, assuming they exist at the same simulation time. Event lists are created at the end of the process, containing information detailing interactions between each object. A "Schrödinger's Cat" approach [16] is used in post-processing to exclude any objects and breakups that don't belong within the scope of a given scenario.

2.1 Future Population Model

The IPM and FLM used in this study were developed using the same methodology as previous ADEPT studies and are described in depth in [7]. The IPM includes all known catalog objects along with a set of emulated objects representing unknown and subtrackable (<10 cm) objects on orbit. The FLM included in the IPM replicates historical launch traffic for different orbital regimes, including continuously replenished constellations (CRCs), non-CRCs, and non-constellation objects.

A future constellation model (FCM) containing multiple large LEO constellations (LLCs) is added to the FLM. These constellations represent future proposed systems gathered from public data, including Federal Communications Commission (FCC) filings. A comprehensive breakdown of the FCM model in presented in [9]. The constellations and launch traffic included in the FLM are consistently maintained throughout the simulation, creating a constant flux of satellite disposal and replenishment.

2.2 Scenario Definitions

Scenarios are used within ADEPT's post-processing program to define the future traffic and debris mitigation behaviors modeled in each future environment simulation. The traffic level defines what subset of FCM are to be included in the simulation. At a given traffic level, scenario variants are made by modeling different debris mitigation behaviors such as post-mission disposal (PMD) success rate or control-to-reentry (C2R). PMD success rate affects the amount of future traffic that successfully reaches its disposal altitude or completes C2R. PMD success rate varies within the set {50, 60, 70, 75, 80, 85, 90, 95, 99, 100}. C2R refers to a disposal method where operators continue to maintain control over satellites after disposal. This practice allows satellites to maintain the ability to perform collision avoidance (COLA) maneuvers during disposal, effectively eliminating the risk of collision for these objects. In this study, over 1,200 future environment scenarios are simulated, each with some unique combination of traffic level, PMD success rate, and C2R usage. Analyzing such an extensive scenario set is necessary to thoroughly examine the consequences that different operational behaviors have on the environment.

The traffic levels used here have been described in depth in previous studies [7,8,9]. A detailed breakdown of the number and distribution of satellites for each traffic level is provided in Appendix A. The "Baseline" scenario set is defined to model a level of traffic comparable what is currently on orbit. "No-New" and "FCM-All" sit on the extreme ends of the future traffic spectrum, including 0% and 100% of all FCM constellations, respectively. "Intermediate" scenarios model incremental steps in activity level ranging from "Baseline" to "FCM-All" while maintaining a balanced distribution of traffic throughout LEO. The "Projection" scenarios behave similarly by successively adding FCM constellations by operator. Other traffic scenarios examine the effects of imbalanced traffic in high and low LEO. Finally, "Tiered-Deorbit" scenarios are used to evaluate the effectiveness of a varied ruleset for satellite disposal.

3 UNCONTROLLED MASS PER YEAR

UMPY was initially developed to characterize the "levels of activity" modeled in different future traffic scenarios. It was important for UMPY to create strong correlations between scenario activity levels and different environmental metrics while being computationally simple. By doing so, scenarios can easily be compared to each other in bulk to study the environmental consequences of different operational behaviors in a robust manner.

In short, UMPY is the summation of each uncontrolled object's mass after scaling by a factor related to the fraction of simulation time that the object exists on-orbit. This summation is divided by the simulation duration to calculate the average amount of uncontrolled mass left on-orbit per year throughout a simulation. Evaluating activity on a per-year basis also allows for studying the effects of continuous replenishment and disposal by large constellations.

Fig. 1 shows the relationship between UMPY and the size of the total and trackable object population on orbit at the end of the simulation. Each data point represents the average value across 100 Monte Carlo runs for an individual scenario. In total, the results of over 1,200 scenarios are plotted in Fig. 1. UMPY values range from roughly 27,000 kg/yr to over 150,000 kg/yr across the full slate of future traffic scenarios.

As seen in Fig. 1, UMPY and object count are strongly correlated. There is relatively little variation in population growth amongst scenarios with similar UMPY values. This means that given the UMPY value of a given scenario, the size of the debris population can be estimated through Fig. 1. For example, a scenario with an UMPY value of 90,000 kg/yr should roughly expect number of objects larger than 1 cm to reach 1 billion after 100 years, with around 20 million of those objects being trackable.

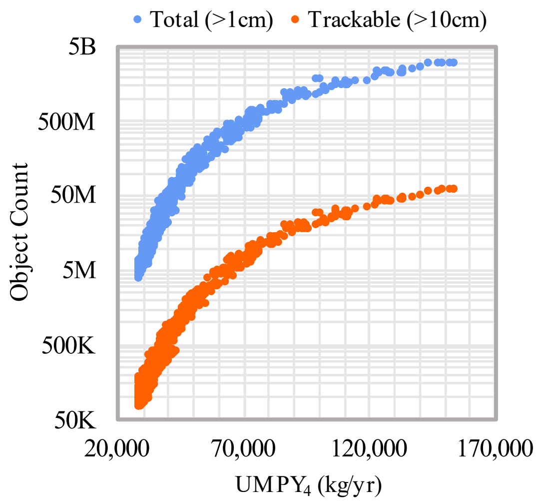

Figure 1. Object population sizes in 2120 as a function of $UMPY_4$ across all scenarios

Previous ADEPT studies [8] have shown similar correlations to other environmental metrics, including collision rates, conjunction frequencies, and launch window closures. Furthermore, these correlations have been leveraged to show that constellation operators can target specific UMPY values by modifying debris mitigation methods to achieve desired environmental effects [9].

The version of UMPY presented here was developed in 2023 [8] as an improvement on previous versions. UMPY has changed significantly from its initial formulation [5], with each iteration improving upon the last. The following subsections will explore each of the different factors that shaped the current form of UMPY.

3.1 Parameter Selection

The first step of developing an environmental index is deciding which parameters to consider. Potential parameters should relate to various aspects affecting the debris environment, including physical spacecraft properties, orbital parameters, mission strategies, and mitigation behaviors. The best parameters to use will vary depending on the intended level of complexity and purpose behind the index.

The goal of creating UMPY was to create a computationally simple index that can characterize the broad operational activity levels exhibited within a single future environment simulation. Working towards this goal, the simplest starting point is to consider the number of failed satellite disposals per year. Scenarios with the most future constellation activity should also have the highest number of satellite disposal failures, especially with low PMD success rates. Large amounts of debris in non-compliant disposal orbits should directly cause higher collision rates and increased debris growth.

Satellite area and mass are also considered as candidate parameters. Both parameters have been shown to correlate with the degradation of the LEO environment [17,18] and are used in many different indices. The area of a failed satellite is directly related to its probability of being involved in a collision. Large amounts of undisposed mass should also lead to debris growth as mass is directly related to the number of fragments produced in an on-orbit breakup [19].

These three parameters are uncomplicated and should hold a lot of explanatory power. Size, mass, and area data are easily accessible for most constellations and does not require any additional modeling or estimation to incorporate. The parameter that best correlates with various environmental metrics can be identified by comparing each candidate across multiple future traffic scenarios.

Eq. 1 describes the general form of the three Undisposed Parameter per Year (UPPY) indices examined in this subsection. t_{sim} is the simulation duration (100 years), n_{fail} is the number of failed satellites on orbit, and P_i is the respective value of each candidate parameter for a given satellite. In other words, P_i is equal to either the object's count, area, or mass.

$$UPPY = \frac{1}{t_{sim}} \sum_{i=1}^{n_{fail}} P_i \tag{1}$$

Fig. 2 shows the total object count after 100 years for each scenario. The "level of activity" in each scenario is measured through the UPPY index described by Eq. 1 for each candidate parameter: object count, area, and mass. The correlations between UPPY and total object count are very similar, regardless of the parameter used. The data suggests a quadratic relationship, as shown by each trendline; however, there is a significant amount of variance displayed in each plot. For example, scenarios that model roughly 2,000 undisposed satellites per year

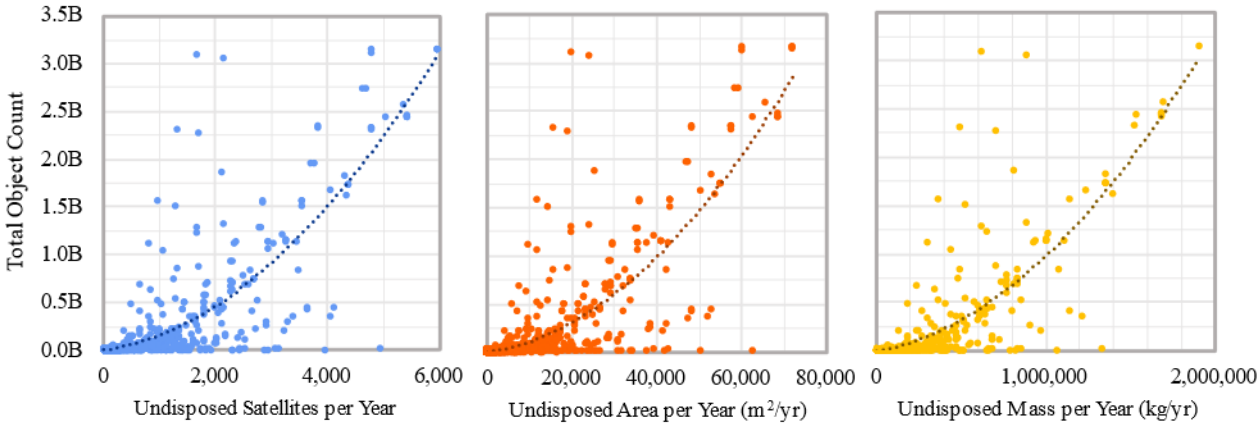

Figure 2. Correlations between total (>1 cm) object count in 2120 and undisposed object candidate parameters

result in total object counts ranging from 10 million to over 3 billion. This level of variance makes it difficult to truly determine which parameter best correlates to total object count and must be resolved to properly identify the best candidate parameter. Through visual inspection, the variance seen throughout Fig. 2 does not appear to be randomly distributed. This suggests that there is some mechanism that is not considered in the UPPY formulation.

Examining the outlier scenarios in Fig. 2 reveals the effect of altitude on the total object count. This effect is shown in Fig. 3, which highlights two sets of future traffic scenarios using the undisposed satellite data set plotted in Fig. 2.

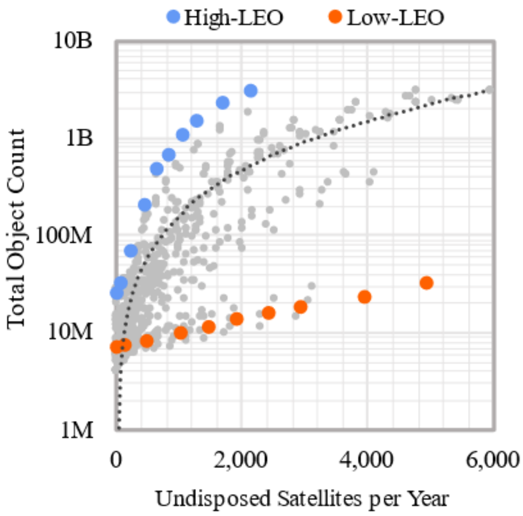

Figure 3. Effect of altitude distribution on total (>1 cm) object count in 2120

The High-LEO and Low-LEO scenarios model the effect of having an imbalance in traffic in high-LEO (>800 km) and low-LEO (<600 km), respectively. Each data point within a scenario set uses the exact same future traffic model but differs in PMD success rate. A logarithmic scale is used on the y-axis to better display the effect of improving PMD success rate within a given scenario.

The PMD trends within the High-LEO and Low-LEO scenarios appear to follow a curve somewhat resembling the trend across the full scenario set. This suggests that the UPPY formulation over-emphasizes the contribution of objects in low-LEO while under-emphasizing those in high-LEO.

Eq. 2 was developed to improve on the UPPY formulation in Eq. 1 using these new insights. The UPPLY (Undisposed Parameter per Year - Lifetime) equation scales the value of each candidate parameter by the ratio of the object's lifetime, $life_i$, to the simulation duration t_{sim}. Note that lifetime here refers to the number of years an object spends on orbit within the simulation. This modification reduces the contribution of objects that fail at low altitudes and re-enter in a few years. These objects still pose a risk to the environment, but that risk is partially reduced due to the natural cleaning effect of the atmosphere. On the other hand, objects that fail at higher altitudes may remain on orbit for the full simulation. These objects pose a risk over a prolonged period fully and fully contribute to UPPLY.

$$UPPLY = \frac{1}{t_{sim}} \sum_{i=1}^{n_{fail}} P_i \frac{life_i}{t_{sim}} \tag{2}$$

The correlations for each parameter can now be reassessed using the UPPLY formula. Fig. 4 displays the relationship between total object count and each of the three UPPLY indices. Introducing the lifetime scaling factor $life_i/t_{sim}$ dramatically reduces the variance in the object count trends compared to the results shown in Fig. 2. A quadratic line of best fit is plotted for each index, with their respective R^2 and residual sum of squares (RSS) values listed. Of the three indices, the undisposed mass index has the lowest RSS value, which signifies that it has the strongest correlation to total object count.

However, total object count is just one measure of the LEO debris environment. The best parameter should be strongly correlated to multiple environmental metrics. To do this, each of the three indices are re-evaluated using a new metric, trackable collision count. The trackable collision count measures the cumulative number of collisions between two trackable objects over the 100-year simulation. Fig. 5 plots the relationship between trackable collision count and the three UPPLY metrics. Once again, undisposed mass has the strongest correlation as shown through comparing RSS values.

Overall, UPPLY shows the strongest correlations when using mass as the candidate parameter. UMPLY (Undisposed Mass per Year - Lifetime) will therefore be used as the basis for comparison in the following sections.

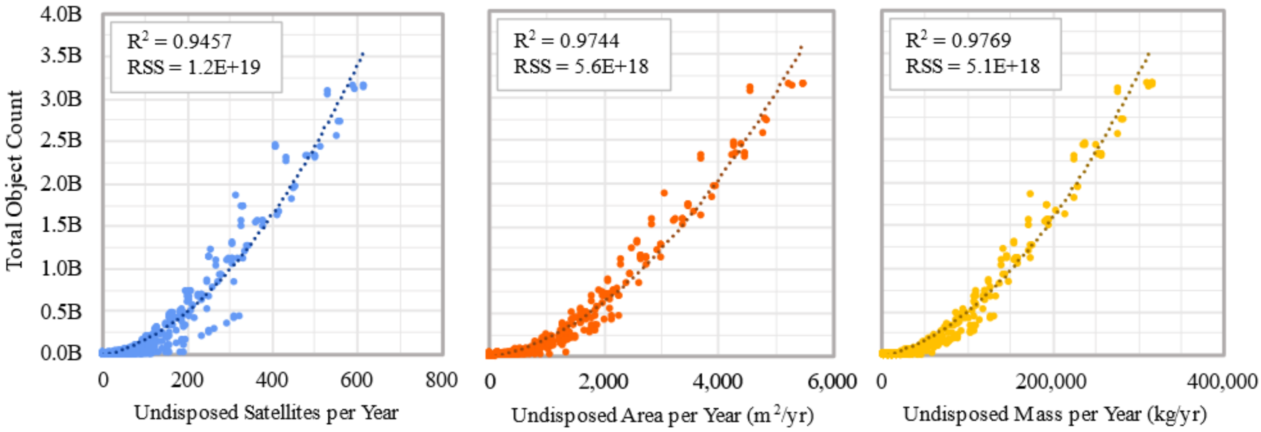

Figure 4. Correlations between total (>1 cm) object count in 2120 and undisposed object candidate parameters after adjusting for object lifetime

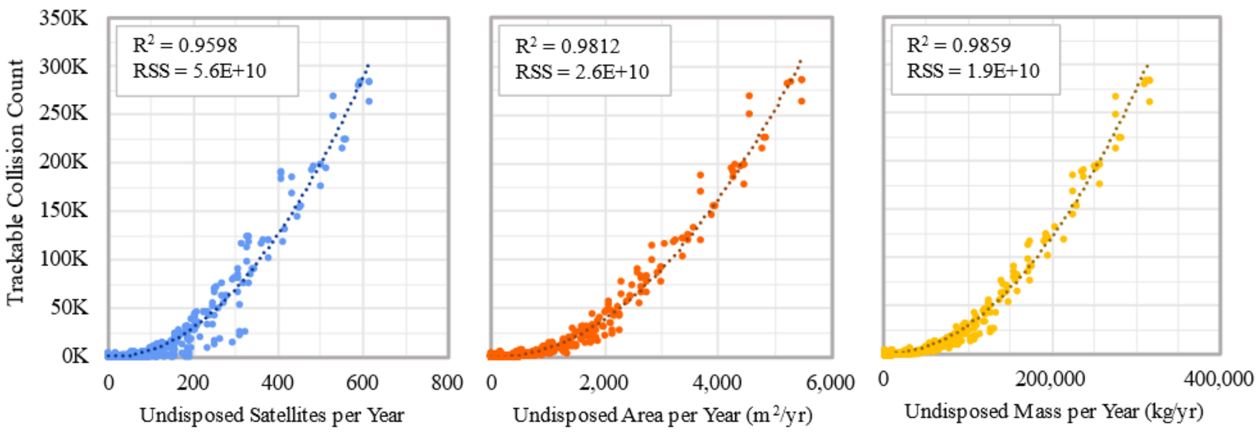

Figure 5. Correlations between cumulative trackable (>10 cm) collisions over 100 years and undisposed object candidate parameters after adjusting for object lifetime

3.2 Lifetime vs. Altitude

Results from the previous section demonstrated that considering the amount of time an object spends on orbit is a necessary to accurately measure the activity level of a given scenario. Scaling the contribution of each candidate parameter by the lifetime fraction $life_i/t_{sim}$ drastically improved the correlations between activity level and environmental impact.

While there was a demonstrable benefit to incorporating lifetime into the UPPLY formulation, it is important to explore other parameters to validate this decision. Since lifetime was introduced to consider the effects of traffic imbalances in high and low LEO, an obvious choice for an alternate parameter is altitude. In this section, two new indices will be introduced and compared to the UMPLY index defined by Eq. 2.

UMPAY is defined by Eq. 3 as a modification to UMPLY. UMPAY scales the mass contribution of each undisposed object by the altitude factor A_i, given by Eq. 4. The altitude scaling factor is equal to some fractional value for all satellites that fail between 340 km and 650 km. Any failures above 650 km fully contribute to UMPAY while objects that fail below 340 km are ignored due to their rapid re-entry times.

$$UMPAY = \frac{1}{t_{sim}} \sum_{i=1}^{n_{fail}} m_i A_i \tag{3}$$

$$A_i = \begin{cases} \left(\frac{alt_i - 340km}{310km}\right)^2, & 340km \leq alt_i \\ 1, & 650km < alt_i \end{cases} \tag{4}$$

Partial Uncontrolled Mass per Year (PUMPY) is described by Eq. 5 and does not incorporate any type of scaling factor. Instead, PUMPY only considers the mass of satellites that failed above 650 km. Failures below 650 km are ignored.

$$PUMPY = \frac{1}{t_{sim}} \sum_{i=1}^{n_{fail}} m_i \tag{5}$$

Fig. 6 compares the correlations between UMPLY, UMPAY, and PUMPY to total object count. Of the three indices, UMPAY displays the worst correlation. This is an interesting result considering the similarity between UMPAY and PUMPY. Both indices sum the full mass of each failed object above 650 km and completely ignore failures below 340 km. This indicates that the discrepancy between UMPAY and PUMPY altitude scaling factor is caused by the altitude scaling factor, A_i. Modifications to the altitude and exponent values in the Eq. 4 could likely improve the efficacy of the UMPAY formula; however, efforts to optimize the altitude scaling factor may not be worthwhile given the performance of the lifetime scaling factor.

Overall, UMPLY outperforms the other two indices, as indicated the RSS values listed in each plot. This validates the decision in the previous section to incorporate lifetime as a parameter instead of altitude.

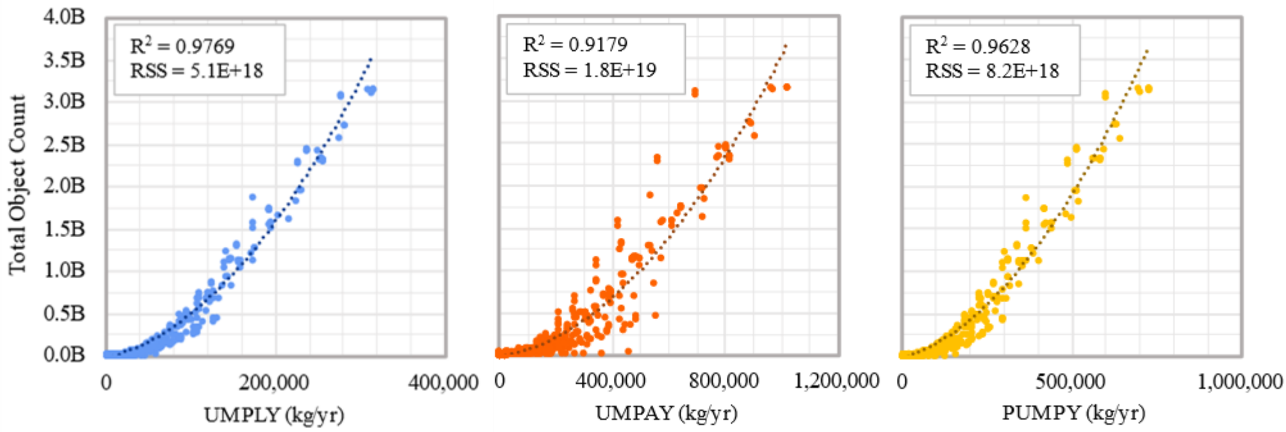

Figure 6. Effect of lifetime and altitude scaling on correlations with total (>1 cm) object count in 2120

3.3 Accounting for Disposed Objects

Each of the indices introduced in the previous sections only account for satellites in non-compliant disposal orbits. While failed objects do contribute significantly to the degradation of LEO, they are not the only objects that pose a risk to space traffic. Successful disposal does significantly reduce the collision risk of an object relative to being undisposed; however, the risk is not eliminated in its entirety. This difference is evident when comparing the effects of unsuccessful, successful, and C2R disposal methods on the environment. In ADEPT, objects using a C2R disposal method can perform COLA maneuvers and are treated as operational objects.

The relationship between UMPLY and trackable collisions is shown in Fig. 7. New C2R copies of each scenario are added to the plot in addition to the scenario data shown previously. The uncontrolled and C2R disposal results for a single future traffic scenario are highlighted. Logarithmic axes are used to better display the difference in outcomes between the two disposal methods.

As described for Eq. 2, the only objects included in the UMPLY summation are those left undisposed. This means that UMPLY is agnostic to the disposal method used by any properly disposed object. Therefore, any two scenarios using the same future traffic model and PMD success rate will always have equivalent UMPLY values, regardless of disposal method. This behavior is depicted in Fig. 7 through the vertical pairs of uncontrolled and C2R disposal scenarios. Both scenarios in each pair have identical UMPLY values, despite resulting in different environmental outcomes. This difference between the two disposal methods is most evident at higher PMD success rates and thus generally lower UMPLY due to the larger number of objects performing COLA maneuvers.

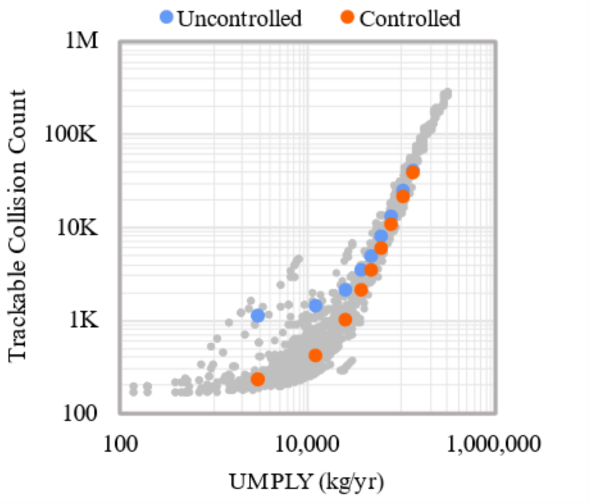

Figure 7. Effect of "control-to-reentry" disposal methods on the cumulative trackable (>10 cm) collision count after 100 years

Rather than only considering the environmental impact of undisposed objects, UMPLY can be modified to instead consider all uncontrolled objects. The equation for $UMPY_0$ is given by Eq. 6, where n_{obj} is the number of uncontrolled objects on orbit. This simple modification adds the ability to evaluate the environmental impacts of different disposal methods.

$$UMPY_0 = \frac{1}{t_{sim}} \sum_{i=1}^{n_{obj}} m_i \frac{life_i}{t_{sim}} \tag{6}$$

An example is provided in Tab. 1 to illustrate the difference between UMPLY and $UMPY_0$. Consider a constellation of 100 satellites with masses of 350 kg. Three different disposal methods are evaluated: a 25-year uncontrolled disposal, a 5-year uncontrolled disposal, and a 5-year C2R disposal. PMD success rate is set at 90% for each method. Since UMPLY only accounts for undisposed objects, the constellation UMPLY is 17.5 kg/yr regardless of disposal option. On the other hand, $UMPY_0$ reveals the successive improvements made by each disposal method. The 5-year disposal method does not contribute as much to $UMPY_0$ as the 25-year method due to the shorter lifetimes of uncontrolled objects. The C2R disposal method performs even better since all successfully objects remain controlled through reentry.

Table. 1 Constellation disposal method comparison (n_{sats} = 100, m = 350kg, PMD = 90%, $life_{fail}$ = 50 yrs)

Disposal Method	UMPLY (kg/yr)	$UMPY_0$ (kg/yr)
25-Year Uncontrolled Disposal	17.5	96.25
5-Year Uncontrolled Disposal	17.5	33.25
5-Year Control to Reentry	17.5	0

The correlation between $UMPY_0$ and trackable collisions is presented in Fig. 8. As expected, scenarios modeling C2R disposal methods have lower $UMPY_0$ values compared to their uncontrolled equivalents. At lower PMD success rates, C2R provides only a marginal benefit over uncontrolled disposals. In these cases, the benefit of C2R is mostly overshadowed by the enormous negative consequence of having high failure rates. On the other hand, the benefits of C2R are clearly visible at higher PMD success rates. With uncontrolled disposals, the marginal benefit of improving PMD success rate sharply drops off above 90%. Employing C2R brings additional improvements to mitigation that cannot be reached through uncontrolled reentry alone.

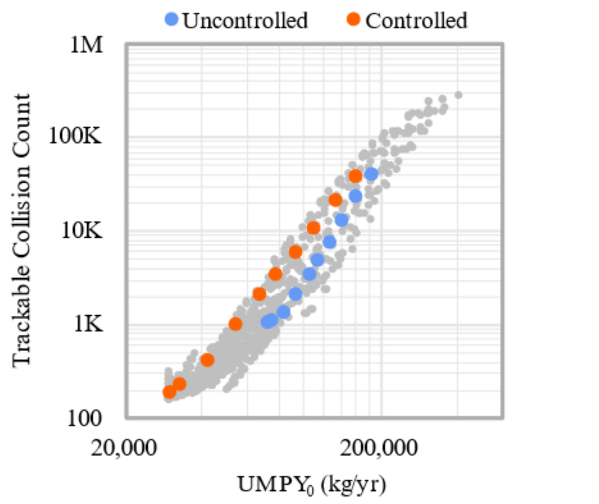

Figure 8. Relationship between $UMPY_0$ and cumulative trackable (>10 cm) collision count after 100 years

3.4 Non-Linear Lifetime Weighting Factor

One consequence of accounting for all uncontrolled mass is the increase in variance between $UMPY_0$ and various environmental metrics. This is seen in Fig. 9 where at an $UMPY_0$ value of 100,000 kg/yr, the number of trackable objects ranges from 200 thousand to over 4 million. Once again, two scenario sets are highlighted to examine if there is some effect of lifetime that remains uncaptured.

Re-examining the High-LEO and Low-LEO scenario sets shows that improvements to PMD success rate reduces trackable object growth at a faster rate for constellations at higher altitudes than lower altitudes. This suggests that object lifetime has some higher order effect on the environment that is not currently captured by UMPY_0.

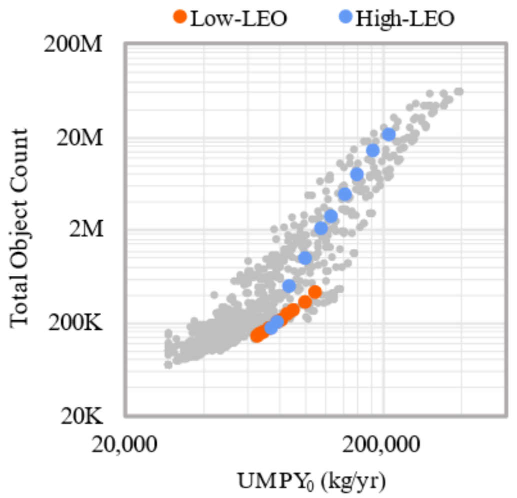

Figure 9. Trackable (>10 cm) object count in 2120 compared to $UMPY_0$

A new lifetime scaling factor, given by Eq. 7, was developed to better capture the non-linear relationship between altitude, lifetime, and collision probability. The degree of non-linearity modeled in Y_i is dependent on the exponential parameter X. As X increases, the contribution of objects with shorter lifetimes is increasingly diminished relative to those with longer lifetimes. Eq. 8 defines the new equation for UMPY which replaces the linear scaling factor $life_i/t_{sim}$ with the new non-linear lifetime scaling factor. Note that as X approaches 0, Eq. 8 approaches UMPY_0.

$$Y_i = \frac{e^{X\left(\frac{life_i}{t_{sim}}\right)} - 1}{e^X - 1}, \quad X \geq 0 \tag{7}$$

$$UMPY_X = \frac{1}{t_{sim}} \sum_{i=1}^{n_{obj}} m_i Y_i \tag{8}$$

The relationship between UMPY_X and different environmental metrics is dependent on the selection of X. Too low of an X value will under account for the effect of lifetime, while a value that is too high will lead to an overcorrection. One method for selecting X is to statistically evaluate which value leads to the lowest amount of variance relative to some regression model; however, there are difficulties with that approach in this context. As X increases, the UMPY_X value of each scenario decreases by some amount related to the number of uncontrolled, low-LEO objects being modeled. This causes the distribution of UMPY_X values to become increasingly positively skewed with increasing X. Properly accounting for this requires using a statistical method that is more advanced than simply comparing RSS values, as done previously.

Instead, a heuristic approach is taken to estimate the best exponential parameter value. At the ideal value of X, Y_i will best account for the long-term environmental risk posed by an uncontrolled object. When this occurs, the variance between UMPY_X and the given environmental metric will be at a minimum, resulting in the trends across different scenario sets to be aligned. The best value of X can then be approximated by visually comparing UMPY_X plots for varying X. This process is depicted in Fig. 10.

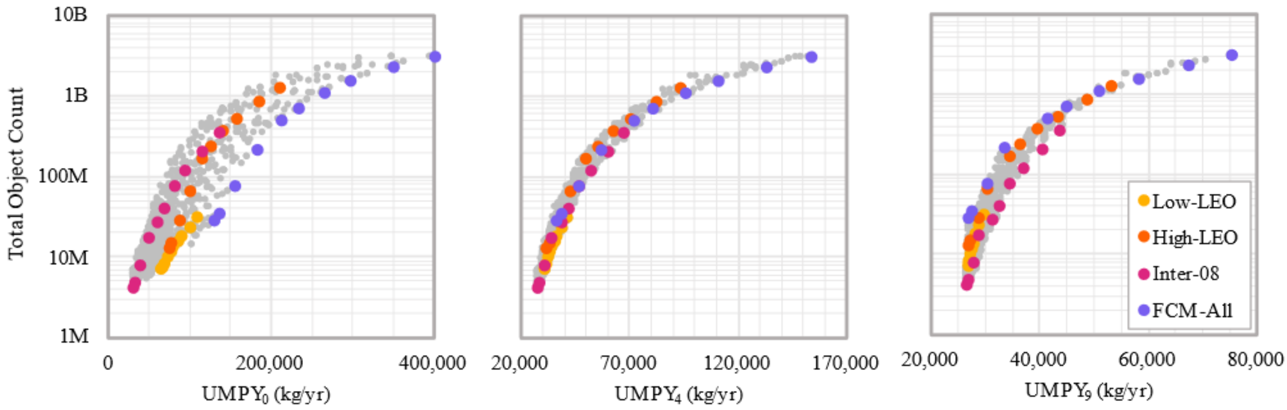

Figure 10. Effect of varying X on relationship between and $UMPY_X$ and total (>1 cm) object count in 2120

The relationship between total object count and UMPY_X is plotted in Fig. 10 for three values of X. Four sets of scenarios are highlighted to visualize the relative shift in scenario trends as X varies. While not depicted here, 10 values of X were examined, using integers ranging from 0 to 9. UMPY_0 and UMPY_9 are the boundary indices, representing cases where the effect of lifetime is undercompensated and overcompensated, respectively. After examining each of the 10 other indices, $UMPY_4$ was found to correlate best to total object count. As X increases from 0 to 4, the trends across each set of scenarios begin to align, leading to a reduction in variance. Increasing X beyond a value of 4 causes the scenario trends to shift past alignment, increasing variance. This behavior is most evident when comparing the relative positions of the Inter-08 and FCM-All scenario sets across each subplot within Fig. 10.

The same process was repeated to study whether different exponential parameter values work better for different metrics. Fig. 11 shows the relationship between trackable object count and $UMPY_4$, which provides the strongest correlation compared to when using other values of X. Examining the relationship with cumulative trackable collisions in Fig. 12 presents a slightly different result, where an exponential parameter value of 3 provides the strongest correlation.

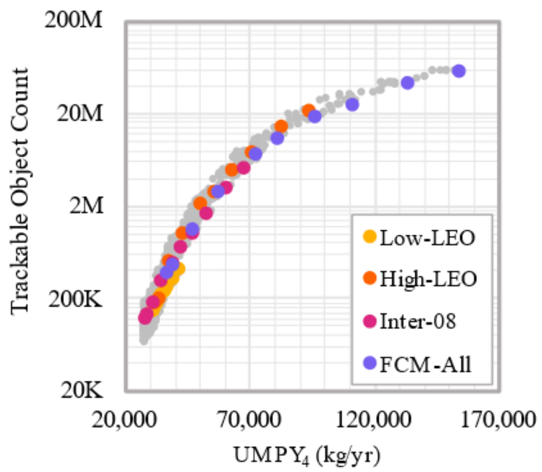

Figure 11. Trackable (>10 cm) object count in 2120 compared to $UMPY_4$

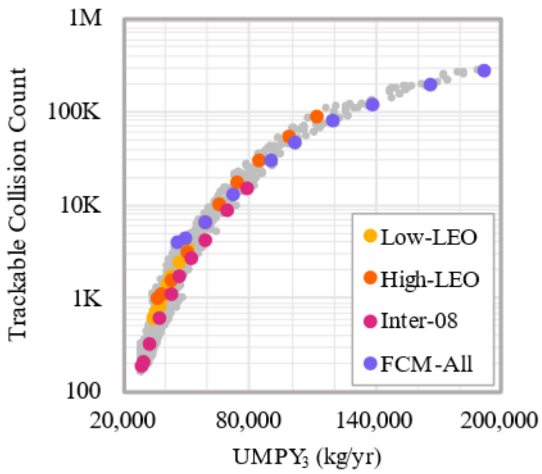

Figure 12. Cumulative trackable (>10 cm) collision counts over 100 years compared to $UMPY_3$

4 COMPARISON TO OTHER INDICIES

Dozens of indices have been developed to quantify the impact that certain objects or constellations may have on the LEO environment. In this section, three indices will be evaluated to see how well they correlate behaviors to environmental outcomes compared to simulation results UMPY. The first two indices are simple composite metrics that quantify environmental risk by summing the number of object-years and kilogram-object-years on orbit. The third index measures orbital capacity based on the Collision Risk Balance Model developed by McKnight and Dale [20].

Unlike UMPY, which quantifies the level of activity in a future traffic scenario over time, these indices have been used to quantify the state of the environment at a single moment in time. While there are many potential ways to measure scenario activity across multiple years through these indices, this section takes the approach of calculating the average index value across the full simulation for each scenario.

The goal of this section is to leverage the results of over 1,200 ADEPT future environment simulations to examine how well each index captures the environmental consequences of different operational behaviors, as is done with UMPY. It is important to note that while done as faithfully as possible, the implementation of these indices may differ in scope from the original intentions of their respective creators.

4.1 Regulatory Composite Metrics

Object-years has been used by both the FCC [21] and the United States Government [22] in regulations requiring satellite operators to limit the production of uncontrolled or mission related debris in LEO. Related is the kilogram-object-year composite metric, which was developed due to concerns with the efficacy of the object-years approach. Object-years and kilogram-object-years respectively sum the lifetime and the lifetime-mass product of each uncontrolled object on orbit.

Fig. 13 compares the correlations that object-years, kilogram-object-years, and $UMPY_4$ have with total object count. Fig. 14 shows a similar comparison using the cumulative number of trackable collisions as the environmental metric. The object-year and kilogram-object-year values for each scenario represent the average index value throughout the simulation. For both environmental metrics, UMPY has the strongest correlation of the three indices.

Comparing the kilogram-object-years plot in Fig. 13 to the $UMPY_0$ plot in Fig. 10 shows that the two indices perform nearly identically. The reason for this is clear after revisiting Eq. 6. Both kilogram-object-years and $UMPY_0$ multiply the mass contribution of each object by its lifetime; however, in the $UMPY_0$ summation, lifetime is divided by the simulation time. In other words, the $UMPY_0$ value of a given scenario is simply the by average kilogram-object-years on-orbit divided by t_{sim}. Given this knowledge, the improvement in correlation with $UMPY_4$ over kilogram-object-years is therefore strictly due to the non-linear lifetime factor. This suggests that the kilogram-object-years approach does not capture the relationship between lifetime and collision likelihood as well as is done with $UMPY_4$.

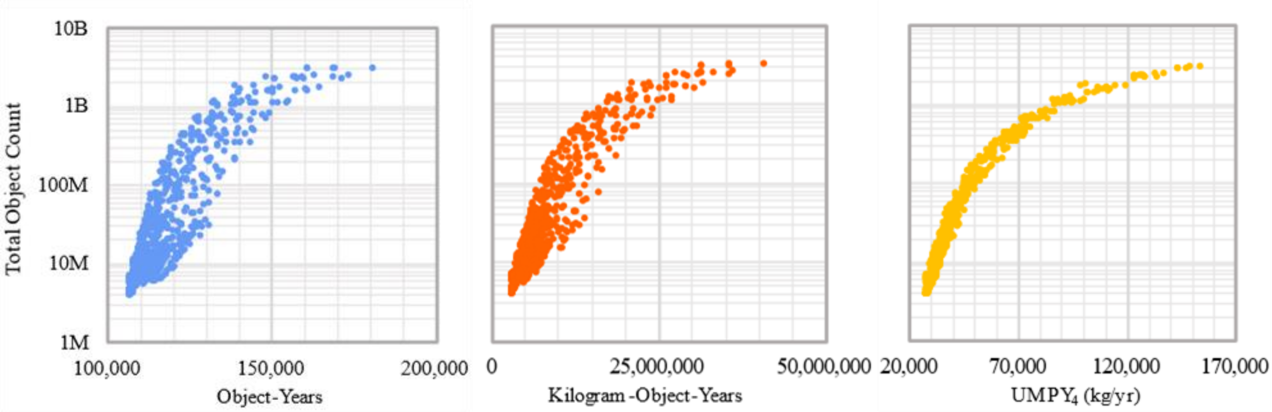

Figure 13. Comparing correlations for object-years, kilogram-object-years, and $UMPY_4$ with total (>1 cm) object count in 2120

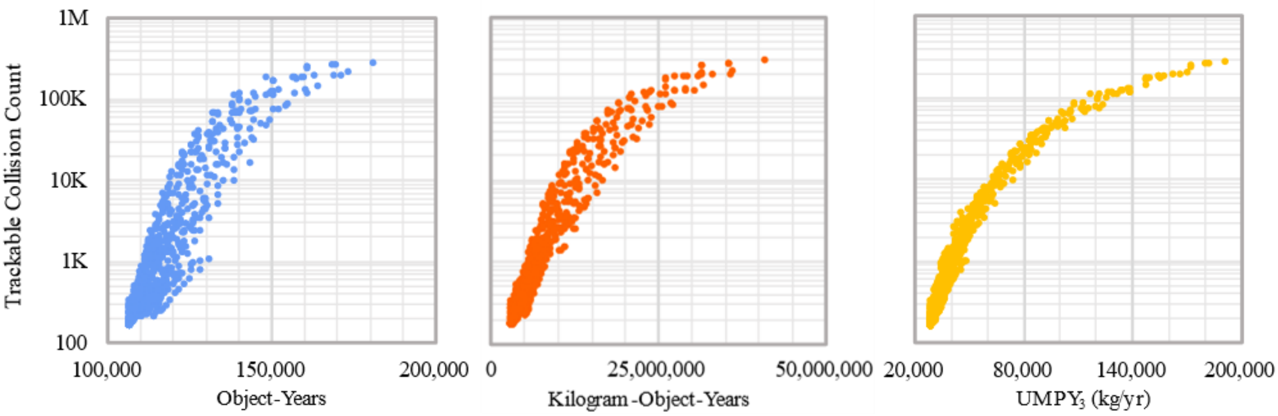

Figure 14. Comparing correlations for object-years, kilogram-object-years, and $UMPY_3$ with cumulative trackable (>10 cm) collision count

4.2 Collision Risk Balance Model

McKnight and Dale developed the Collision Risk Balance Model [20] as a method for quantifying orbital capacity by considering an object's risk burden, capacity for risk reduction, and persistence on orbit.

Risk burden posed (RBP) represents the collision risk posed by an object and is defined by Eq. 9 as the product of an object's mass and area.

$$RBP_i = m_i A_i \tag{9}$$

Risk burden abated (RBA) is described by Eq. 10 and represents the ability of an operational satellite to reduce its collision risk. RBA is a function of an object's maneuverability (*MAN*), risk reduction maneuver threshold (*RMM/PC*), and collision risk abatement goal (*AbPC*). Detailed definitions of those parameters are described in [20], along with a table of values. Note that RBA is 0 for all uncontrolled objects as, by definition, these objects have no maneuver capabilities.

$$\begin{aligned} &RBA_i \\ &= 2.15\{0.33MAN_i\} \\ &\times 2.15\left\{1-\left(\frac{[6+\log_{10}(RMM/PC_i)]^2}{10}\right)\right\} \\ &\times 2.15\left\{1-\left(\frac{[7+\log_{10}(AbPC_i)]^2}{10}\right)\right\} \end{aligned} \tag{10}$$

The values for *MAN*, *RMM/PC*, and *AbPC* used in this study are listed in Tab. 2. Operational satellites within the start catalog and non-CRC populations use the default parameter values suggested by McKnight and Dale. CRC satellites use different *RMM/PC* and *AbPC* values depending on the specific operators being modeled. Finally, all FCM satellites use the lowest *RMM/PC* and *AbPC* thresholds to reflect the high maneuver capabilities of modern LLC operators.

Table. 2 Risk burden abatement parameters for operational satellites

Population	MAN	RMM/PC	AbPC
Catalog Operational	3	5E-4	1E-5
Non-CRC	3	5E-4	1E-5
CRC 1-3	3	1E-4	3.2E-6
CRC 4-5	3	1E-5	1E-6
FLM	3	1E-5	1E-6

The altitude adjustment (AA) factor, given by Eq. 11, is used to scale the contribution of each object to correct for on-orbit persistence.

$$AA_i = 1 + \left(\frac{alt_i - 300\text{km}}{100\text{km}}\right)^{3.85} \tag{11}$$

Eqs. 9, 10, and 11, describe each of the three risk considerations used in the Collision Risk Balance Model. Eq. 12 defines orbital capacity (OC) through these considerations, where n_{obj} is the total number of IPM objects within the scenario. Note that orbital capacity is treated as unitless.

$$OC = \sum_{i=1}^{n_{obj}} RBP_i * (10 - RBA_i) * AA_i \tag{12}$$

Fig. 15 shows the correlation between orbital capacity and total object count. Here, orbital capacity is measured as the average orbital capacity over the full simulation. Overall, the correlation between total object count and orbital capacity is weak. At a given orbital capacity value, the total object count can vary by one to two orders of magnitude.

Five different scenarios are highlighted to identify any hidden trends. Doing so reveals that each scenario appears to be horizontally aligned within the aggregate collection of scenarios. This is most evident when comparing the FCM-All and Inter-11 scenario sets. These two sets have very similar object count numbers for each pair of PMD scenarios. Despite this, the orbital capacity values differ by roughly 60 billion for each pair. Given the similarity in outcomes, the difference in orbital capacity values between the two scenario sets should ideally be much smaller. Similar behavior occurs when examining collision counts.

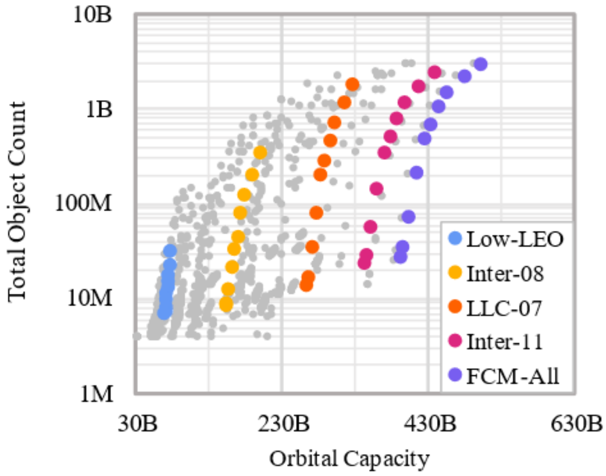

Figure 15. Relationship between total (>1 cm) object count in 2120 and orbital capacity as measured through the Collision Risk Balance Model

Appendix A details the number and distribution of objects at each traffic level. Examining these details reveals that orbital capacity values are heavily influenced by the specific combination of LLC traffic modeled. In particular, the LLC-07 constellation consumes a disproportionate amount of orbital capacity due to the large number of massive satellites in high-LEO. Examining Fig. 15 shows that the orbital capacity values of the Inter-08 scenarios are significantly lower than those of the LLC-07 scenarios, despite having more satellites in each region of LEO. This indicates that orbital capacity is more closely related to the specific LLC objects modeled in the scenario rather than the environmental impacts of the LLC objects.

It is important to emphasize that differences in modeling assumptions between this work and the original source can significantly affect the results. Two instances of modeling differences are described here.

The altitude adjustment factor, AA_i, and the lifetime scaling factor, Y_i, are both used to account for the non-linear effect of on-orbit persistence on the environment. Despite this similarity, the two factors result in vastly different outcomes. In ADEPT, lifetime is determined by how long an object exists within the simulation. This means that the lifetime of an object may be truncated, depending on how late in the simulation the object exists. This is done to account for the reduced impact an object may have on the simulated environment due to the finite bounds of the simulation duration. This effect does not apply to the Collision Risk Balance Model and is appropriately left unconsidered by the altitude adjustment factor.

The Collision Risk Balance Model accounts for operational satellite risk abatement strategies through Eq. 10. Operational satellites with high levels of maneuverability will consume less orbital capacity than their uncontrolled equivalents. Conversely, operational satellites in ADEPT do not contribute in any amount to the simulated environment as they are excluded from the collision generation process. Including these operational satellites overinflates the orbital capacity relative to the collision activity modeled within the scenario. Future modifications to ADEPT will examine the risk posed by operational satellites

A modified orbital capacity formulation, given by Eq. 13, was developed to correct for the modeling differences between ADEPT and the original Collision Risk Balance Model. First, the altitude adjustment factor was replaced with the non-linear lifetime weighting factor, Y_i, to better account for the simulation duration bounds of ADEPT while still capturing the non-linear effects of on-orbit persistence. Additionally, RBA was removed from the summation. Since operational satellites in ADEPT model perfect abatement and all uncontrolled objects have no abatement capabilities, risk abatement can effectively be modeled by only summing the contributions of uncontrolled objects. RBP remains unchanged within the new formulation.

$$OC_{\text{mod}} = \sum_{i=1}^{n_{obj}} RBP_i * Y_i \quad (13)$$

Note that there are multiple ways to adjust Eq. 12 to account for these modeling differences. The adjustments done to create Eq. 13 were selected through leveraging insights from previous sections of this work. Future work could be done to implement the Collision Risk Balance Model in a manner much closer to the original work.

Fig. 16 shows the relationship between total object count and orbital capacity, after adjusting for modeling differences in ADEPT. The exponential parameter was set to a value of 4 based on the results shown in Fig. 10. Trends across each scenario set appear much more in-family compared to the results in Fig. 15. The stronger correlation makes it much easier to relate the consumption of orbital capacity to its impacts on the environment. For example, at an average modified orbital capacity value of 700,000 per year, the number of objects larger than 1 cm should grow to roughly 100 to 200 million after 100 years. In this way, the modified orbital capacity equation could be used to target specific environmental outcomes, similar to how UMPY can be used.

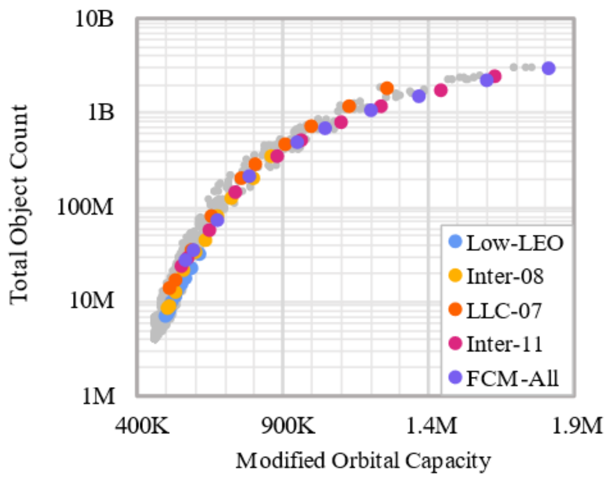

Figure 16. Relationship between total (>1 cm) object count in 2120 and modified orbital capacity

5 CONCLUSION

UMPY was developed as an index to quickly characterize the operational activity exhibited in a future environment simulation. Through UMPY, different scenarios can easily be compared in bulk to study the effects that operational behaviors have on the LEO debris environment. UMPY has evolved over time to produce stronger correlations between scenario activity and various environmental metrics, such as debris population growth and collision rates. This work details the process of developing UMPY from its initial formulation to its current state. This development process can be generally applied to aid in designing other environmental indices.

Mass was shown to better explain the environmental outcomes of future scenario traffic over area and number of failed satellites. To consider the effects of having traffic imbalances between high and low LEO, the mass of each object was scaled by the fraction of time each object exists within the simulation. Furthermore, it was found that the relationship between lifetime and collision likelihood is non-linear. This resulted in the introduction of a non-linear lifetime scaling factor which can be adjusted to improve the correlation between various environmental metrics and scenario activity.

An additional change to UMPY was made to account for the contributions of all uncontrolled objects, rather than just those of undisposed objects. This change gave UMPY the ability to evaluate the environmental impact of different disposal strategies, including reduced disposal lifetimes and C2R methods.

Other composite metric indices were examined to determine how well each index correlates to different environmental metrics compared to UMPY. Object-years and kilogram-object-years were shown to correlate somewhat strongly to object count and collision rates but still exhibited more variance than with UMPY. UMPY was also compared to a modified formulation for orbital capacity, defined by the Collision Risk Balance Model. The modified orbital capacity formulation correlated very strongly with total object count, suggesting that the Collision Risk Balance Model may be very useful in relating orbital capacity consumption to specific environmental outcomes. Future work to improve the implementation of the Collision Risk Balance Model in ADEPT may provide more conclusive evidence of this result.

The analysis completed in this work was made possible through leveraging the results of over 1,200 future environment simulations from ADEPT. Examining such a large collection of scenarios is necessary to properly quantify the relationships between environmental indices and environmental metrics. This ensures that the given index is robust and can account for the environmental impacts brought on by a wide range of operational behaviors.

6 REFERENCES

1. Kessler, D. J., & Anz-Meador, P. D. (2001). Critical Number of Spacecraft in Low Earth Orbit: Using Satellite Fragmentation Data to Evaluate the Stability of the Orbital Debris Environment. *Proc. 3rd European Conference on Space Debris*, ESA SP-473, Darmstadt, Germany.

2. Colombo, C., Letizia, F., Trisolini, M., Lewis, H. G., Chanoine, A., Duvernois, P.-A., Austin, J., Lemmens, S. (2017). Life Cycle Assessment Indicator for Space Debris. *Proc. 7th European Conference on Space Debris,* Darmstadt, Germany.

3. Peterson, G. E. (2012). Target Identification and Delta-V Sizing for Active Debris Removal and Improved Tracking Campaigns. *23rd International Symposium on Space Flight Dynamics*, Pasadena, California, United States.

4. Letizia, F., Colombo, C., Lewis, H. G., Krag, H. (2017). Extending the ECOB Space Debris Index with Fragmentation Risk Estimation. *Proc. 7th European Conference on Space Debris*, Darmstadt, Germany.

5. Henning, G. A., Sorge, M. E., Peterson, G. E., Jenkin, A. B., McVey, J. P., Mains, D. L. (2019). Impacts of Large Constellations and Mission Disposal Guidelines on the Future Space Environment. *Proc. 70th International Astronautical Congress,* IAC-19,18,2,7,x50024, Washington D.C., United States.

6. Henning, G. A., Sorge, M. E., Peterson, G. E., Jenkin, A. B., Mains, D. L., McVey, J. P. (2020). Parameterizing Large Constellation Post-Mission Disposal Success to Predict the Impact to Future Space Environment. *Journal of Space Safety Engineering.* **7**, 171-177.

7. Henning, G. A., Mains, D. L., Maldonado, J. C., Sorge, M. E., Peterson, G. E., Jenkin, A. B., Zundel, J. (2022). Finding the Upper Threshold of LEO Activity that Makes Long-Term Space Operations Unsustainable. *Proc. 73rd International Astronautical Congress*, IAC-24,18,2,2,x69428, Paris, France.

8. Bologna, D. G., Henning, G. A., Sorge, M. E., Peterson, G. E., Mains, D. L., Maldonado, J. C. (2023). Conjunction Frequency-Based Sustainability Assessment of Future LEO Activity. *Proc. 2nd International Orbital Debris Conference*, 6051, Sugarland, Texas, United States.

9. Henning, G. A., Sorge, M. E., Bologna, D. G., Wahleithner, L., Maldonado, J. C. (2024). Correlating LEO Sustainability to Targeted Debris Mitigation Methods Using a Simple Metric. *Proc. 75th International Astronautical Congress*, IAC-24,18,10-E9.4,3,x82761, Milan, Italy.

10. Jenkin, A. B., Sorge, M. E., Peterson, G. E., McVey, J. P., Yoo, B. Y. (2011). 100-Year Low Earth Orbit Debris Population Model. *AAS/AAIA Astrodynamics Specialist Conference,* AAS 11-410, Girdwood, Alaska, United States.

11. Jenkin, A. B., Sorge, M. E., McVey, J. P., Peterson, G. E., Yoo, B. Y. (2013). MEO Debris Environment Projection Study. *Proc. 6th European Conference on Space Debris,* Darmstadt, Germany.

12. Jenkin, A. B., Sorge, M. E., Peterson, G. E., McVey, J. P., (2015). Recent Enhancements to ADEPT and Resulting Sample Projections of the Future Debris Environment. *Proc. 66th International Astronautical Congress,* IAC-15,18,2,2,x28103, Jerusalem, Israel.

13. McClain, W.D. (1977). A Recursively Formulated First-Order Semianalytic Artificial Satellite Theory Based on the Generalized Method of Averaging. *Computer Sciences Corporation, CSC/TR-77/6010*, Greenbelt, Maryland, United States.

14. Jenkin, A. B., & McVey, J. P. (2009) Constellation and "Graveyard" Collision Risk for Several MEO Disposal Strategies. *Proc. 5th European Conference on Space Debris*, ESA SP-672, Darmstadt, Germany.

15. Mains, D. L., & Sorge, M. E. (2022). The IMPACT Satellite Fragmentation Model. *Acta Astronautica*. **195**, 547-555.

16. Henning, G. A., Sorge, M. E., Peterson, G. E., Jenkin, A. B., Mains, D., Maldonado, J. C., Bologna, D. B. (2023). *Proc. 2nd International Orbital Debris Conference*, 6010, Sugarland, Texas, United States.

17. Lewis, H., Radtke, J., Rossi, A., Beck, J., Oswald, M., Anderson, P., Virgili, B. B., Krag, H. (2017). Sensitivity Of The Space Debris Environment To Large Constellations And Small Satellites. *Proc. 7th European Conference on Space Debris*, ESA SP-507, Darmstadt, Germany.

18. Rossi, A., Alessi, E. M., Valsecci, G. B., Lewis, H., Radtke, J., Bombardelli, C., Virgili, B. B. (2017). A Quantitative Evaluation Of The Environmental Impact Of The Mega Constellations. *Proc. 7th European Conference on Space Debris*, ESA SP-356, Darmstadt, Germany.

19. Johnson, N. L., Krisko, P. H., Liou, J.-C., Anz-Meador, P. D. (2001). NASA's New Breakup Model of EVOLVE 4.0 *Advances in Space Research*. **28**(9), 1377-1384.

20. McKnight, D., & Dale, E. (2023). Modelling Empirical Orbital Capacity. *Proc. 2nd International Orbital Debris Conference*, 6069, Sugarland, Texas, United States.

21. Federal Communications Commission. (2022). Request for Orbital Deployment and Operating Authority for the SpaceX Gen2 NGSO Satellite System. 37 FCC Rcd 14882 (16).

22. United States Government. (2019). Orbital Debris Mitigation Standard Practices.

APPENDIX A

Scenario Name	LLCs Included	Total # FCM Sats	Low LEO (<600 km)	Mid LEO (600-800 km)	High LEO (>800 km)
no-new	IPM	0	0	0	0
background	baseline minus some current systems	0	0	0	0
no-llc	baseline – with no replenishment	0	0	0	0
baseline	LO-I + HI-N	5124	3360	0	1764
intermediate-0	baseline + 2 LO	11844	10080	0	1764
intermediate-1	baseline + 4 LO, 3 MID, 3 HI	19135	12800	3060	3275
intermediate-2	baseline + 4 LO, 1 MID, 1 HI	23172	18960	144	4068
intermediate-3	baseline + 6 LO, 6 MID, 4 HI	31211	20772	5000	5439
intermediate-4	baseline + 6 LO, 7 MID, 5 HI	31995	19840	5820	6335
intermediate-5	baseline + 5 LO, 5 MID, 6 HI	32083	20068	5852	6163
intermediate-6	baseline + 6 LO, 2 MID, 2 HI	36360	29520	468	6372
intermediate-7	baseline + 8 LO, 8 MID, 7 HI	44163	28720	5964	9479
intermediate-8	baseline + 9 LO, 7 MID, 7 HI	50206	34384	6222	9600
intermediate-9	baseline + 10 LO, 9 MID, 10 HI	55415	35492	7416	12507
intermediate-10	baseline + 9 LO, 9 MID, 10 HI	62760	40804	6386	15570
intermediate-11	baseline + 10 LO, 14 MID, 14 HI	69038	39828	12140	17070
fcm-all	all proposed LLCs	76606	45668	12140	18798
lo-leo	baseline + all LO and MID LLCs	59572	45668	12140	1764
lo-leo-half	baseline + ½ of all LO & MID LLCs	36392	27812	6816	1764
hi-leo	baseline + all HI LLCs	28878	10080	0	18798
hi-leo-half	baseline + ½ of all HI LLCs	20672	10080	0	10592
fcm-llc1	baseline + LO-ABCDJK + MID-AC	31752	29520	468	1764
fcm-llc2	baseline + HI-LM	9732	3360	0	6372
fcm-llc3	baseline + LO-L + MID-BDEF	9662	4144	3754	1764
fcm-llc4	baseline + LO-EFG + MID-KL	18744	14644	2336	1764
fcm-llc5	baseline + HI-ABQR	6912	3360	0	3552
fcm-llc6	baseline + MID-GHJ + HI-DEF	10794	3360	3564	3870
fcm-llc7	baseline + LO-HMN + HI-GHIJ	18116	9440	0	8676
proj-0	baseline + 3 LO, 2 MID	15080	10864	2452	1764
proj-1	proj-0 + 4 HI	16868	10864	2452	3552
proj-2	proj-1 + 3 MID, 3 HI	22538	10864	6016	5658
proj-3	proj-2 + 4 LO, 2 MID	42446	30304	6484	5658
proj-4	proj-3 + 2 HI	47054	30304	6484	10266
proj-5	proj-4 + 2 LO, 1 MID	53134	34384	8484	10266
proj-6	proj-5 + 4 HI	60046	34384	8484	17178
proj-7	proj-6 + 2 MID	61348	34384	9786	17178
proj-8	proj-7 + 1 HI	62788	34384	9786	18618
proj-9	proj-8 + 1 MID, 1 HI	62986	34384	9804	18798
proj-10	proj-9 + 3 LO, 3 MID	76606	45668	12140	18798
tiered-deorbit-lo	portions of 6 LO, 3 MID, 6 HI	14147	9868	2304	1975
tiered-deorbit-mid	portions of 9 LO, 5 MID, 10 HI	26769	17800	3779	5190
tiered-deorbit-hi	portions of 13 LO, 10 MID, 12 HI	65210	45556	8558	11096